

Numerical and experimental study of the hygric inertia of a hemp-lime concrete

C. Maalouf, M. Lachi, T.H. Mai, E. Wurtz

Abstract— The use of hemp-lime as a construction material combines renewable low carbon materials with exceptional hygrothermal performance. In this paper, the authors study hemp-lime hygroscopic inertia which is the material capacity to adsorb and reject moisture and dampen indoor relative humidity variations. Two experiments are run under isothermal conditions in a hem-lime concrete specimen subjected to static variations of air relative humidity. Only one face of the specimen is in contact with indoor air of a climatic chamber. Other faces are made impermeable to water by adding an alumina sheet. The specimen is weighted each hour. Experimentation is also compared to numerical results that take into account hysteresis phenomenon of the sorption curve under the simulation environment SPARK. Results are also compared to data found in literature for gypsum. The study is also completed by a parametric analysis in order to determine the most important parameters.

KEY WORDS: Hemp concrete, Buffering capacity, modeling, moisture, hysteresis, SPARK.

I. INTRODUCTION

The construction industry is non-sustainable because it is responsible for the consumption of non-renewable raw materials and fossil fuels, and for high CO₂ emissions that impact drastically environment [1]. In order to improve sustainable world's economic growth and improve people's life quality, the use of alternative products such as vegetal fibres (green materials) is necessary [2]. Among these materials, hemp is widely used in building construction. The hemp plant can grow up to 4 m in 4 months with low fertilizer and irrigation demand and all plant parts can be used. Besides, hemp shiv is more resistant to biological decay than other bio-based building materials. When mixing the chopped woody core of the stalks of the hemp plant with lime, it gives hemp concrete a porous ecomaterial with low thermal conductivity [3].

Researches done until this day [4]-[6] allowed us to determine its physical properties and its performances regarding the energy consumption and hygrothermal comfort in buildings. This material show low mechanical properties and is thus mainly used as filling material associated to a wooden structure [7]-[10]. From the thermal point of view,

C. Maalouf, M. Lachi, T.H. Mai are with Laboratoire Thermomécanique- GRESPI, Faculté des Sciences, University of Reims, BP1039, 51687, Reims, France (Corresponding author: chadi.maalouf@univ-reims.fr).

E. Wurtz is with LOCIE FRE CNRS 3220, University of Savoy - 73377, Le Bourget du Lac Cedex, France

hemp-lime mixtures have a low thermal conductivity due to its porous light structure [11]. Its hygric characterization

shows high transfer and storage capacities [12], [13]. In this paper, we are interested experimentally and numerically by its hygric characterization under dynamic conditions and its capacity to store and reject moisture (moisture buffering capacity). First we present experimental results concerning the behaviour of such material under periodical step change of relative humidity. Then results are compared numerically using the simulation environment SPARK, which allows studying coupled heat and moisture transfer through material using Umidus [14] model modified in order to take into account sorption isotherm hysteresis [15]. Results are compared to other materials from literature and mainly to gypsum [16]. Finally a parametric study is run in order to analyze system behaviour.

II. EXPERIMENTAL STUDY

In order to determine moisture buffering capacity, two experiments have been done at laboratory of GRESPI/ LTM of Reims University. The first one considers two samples which surfaces are (10 cm x11 cm) and (12 cmx12 cm) and their thicknesses are 3 cm and 6 cm respectively. The test specimens are exposed to a periodical step change in ambient relative humidity chamber between 75% during 24 hours and 35% during 24 hours (Fig. 1). The temperature is held constant at 20°C. In order to ensure one-dimensional water vapour transfer between the specimen and ambient air, five faces of samples were sealed with an aluminium tape keeping only one face exposed to indoor environmental chamber conditions. The weight change of specimen was measured by a balance with a resolution of 0.01g. Initially, the specimens are in equilibrium state at 20°C temperature and 35% relative humidity. For reasons of availability of the chamber, the period of the tests is 5 days. In order to better determine the behaviour over more a long period, other tests are actually running on.

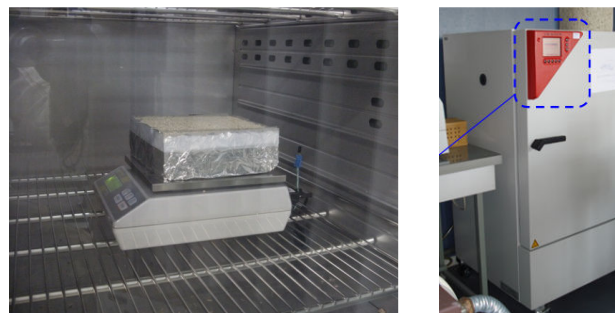


Fig. 1 : View of the samples placed in the climatic chamber.

The second experimental study considers one specimen of hemp concrete of (10 cm x11 cm) and of 6 cm thickness sealed in the same as the first experiment. Initially the

specimen was at 23°C and 30% relative humidity and then it is subjected to a step change of relative humidity to 71% for 24 hours and 30% for the following 24 hours. These conditions were chosen in accordance with data given in [16] in order to compare hemp concrete moisture buffering capacity to gypsum capacity.

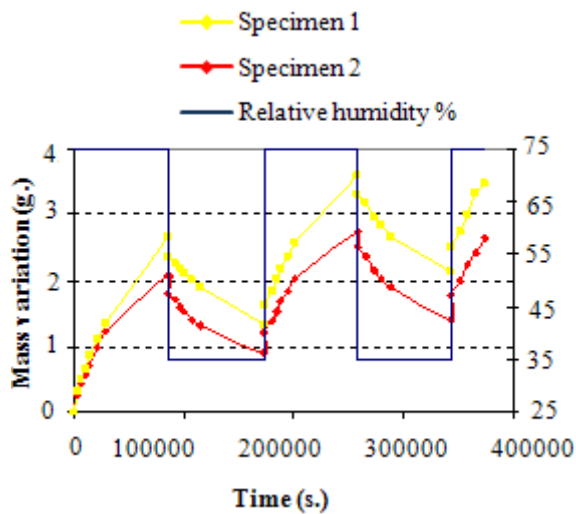


Fig. 2. Mass variation of specimens over a period of 5 days.

Figure 2 shows the variation of the mass in the samples of the first experiment. One can see that for sample 2 thickness 6 cm, the variation of mass are more important than that of sample 1. This means that for over one period of 24:00, the penetration depth in material is higher than 3 cm. The latter is being defined as the depth where the amplitude of moisture content variation is only 1% of the variation on the material surface. It is given by Arfvidsson [17] as:

$$d = 4.61 \sqrt{\frac{D_{\theta} t_p}{\pi}} \quad (1)$$

Where t is time period in seconds. For hemp concrete under a period of 24h and based on [18], $d=3.75$ cm showing that specimen 1 has a thickness lower than penetration depth.

Fig. 3 shows mass variation of the specimen in the second experiment. It has the same trend as in Fig. 2. It should be noted that in this case specimen is initially drier than in case 1 that is why its mass growth is higher. The experimental study is accompanied by a numerical study whose equations of the model are clarified in the following part.

III. PHYSICAL MODEL

We find in the literature several works concerning modeling the hygrothermal transfer. Most of the research is still carried out by using phenomenological macroscopic models, introducing heuristic laws relating thermodynamic

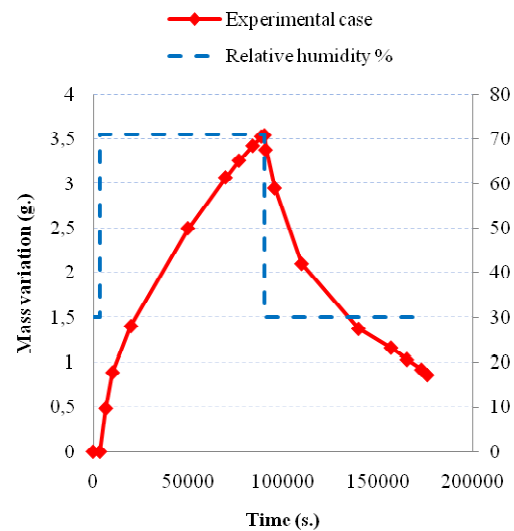


Fig. 3. Mass variation for the specimen in the second experiment over a period of 2 days.

forces to fluxes through moisture and temperature dependent transport coefficient. In this way, one of the most used and accepted macroscopic models for studying heat and moisture transfer through porous material is the Phillip and de Vries model [19] which uses as driving potentials the temperature and moisture content gradient. While most studies on heat transport processes largely agree, no consensus in the choice of driving potentials for describing moisture transport phenomena exists at present and some authors modified the Phillip and de Vries model by using other driving potentials instead of the moisture content. We should cite Perdesen [20] who used the capillary pressure, but in practice it is difficult to be directly measured. Künzel [21] used the relative humidity as a potential. The calculation methodology employed by them is correct since it takes into account the discontinuity phenomenon at the interface.

However, in many circumstances, the direct use of the moisture content as the driving forces can be appropriate since it can be more computationally viable and, most of time moisture content is more useful parameter as it has a simple and direct physic meaning. Consequently, in this paper, we use the Umidus model [14] in which the moisture in porous material can be transported under liquid and vapour phases. The liquid phase is supposed to move by capillary pressure, while the vapor phase is supposed to be diffused due to partial pressure gradients. Considering these hypotheses, the governing moisture balance equation within the wall is given by

$$\frac{\partial \theta}{\partial \tau} = \frac{\partial}{\partial x} \left(D_T \frac{\partial T}{\partial x} \right) + \frac{\partial}{\partial x} \left(D_{\theta} \frac{\partial \theta}{\partial x} \right) \quad (2)$$

The boundary conditions for this equation are given by ($x=0$ and $x=L$):

$$- \rho_l \left(D_T \frac{\partial T}{\partial x} + D_{\theta} \frac{\partial \theta}{\partial x} \right) \Big|_{x=0,e} = h_{M,e} (\rho_{ve,a,e} - \rho_{ve,s,e}) \quad (3)$$

$$-\rho_l \left(D_T \frac{\partial T}{\partial x} + D_\theta \frac{\partial \theta}{\partial x} \right) \Big|_{x=L,i} = h_{M,i} (\rho_{ve,s,i} - \rho_{ve,a,i}) \quad (4)$$

The governing energy balance equation states that the temporal variation of energy is due to the net amount of heat received/lost by conduction and the phase change within pores:

$$\rho_0 C p_m \frac{\partial T}{\partial \tau} = \frac{\partial}{\partial x} \left(\lambda_{app} \frac{\partial T}{\partial x} \right) + L_v \rho_l \left(\frac{\partial}{\partial x} \left(D_{T,v} \frac{\partial T}{\partial x} \right) + \frac{\partial}{\partial x} \left(D_{\theta,v} \frac{\partial \theta}{\partial x} \right) \right) \quad (5)$$

where

$$C p_m = C p_0 + C p_l \frac{\rho_l}{\rho_0} \theta \quad (6)$$

And the boundary conditions for this equation are given by (x=0 and x=L):

$$-\lambda_{app} \frac{\partial T}{\partial x} - L_v \rho_l \left(D_{T,v} \frac{\partial T}{\partial x} + D_{\theta,v} \frac{\partial \theta}{\partial x} \right) \Big|_{x=0,e} = h_{T,e} (T_{a,e} - T_{s,e}) + L_v h_{M,e} (\rho_{ve,a,e} - \rho_{ve,s,e}) + \alpha_e \Phi_{ray,e} \quad (7)$$

$$-\lambda_{app} \frac{\partial T}{\partial x} - L_v \rho_l \left(D_{T,v} \frac{\partial T}{\partial x} + D_{\theta,v} \frac{\partial \theta}{\partial x} \right) \Big|_{x=L,i} = h_{T,i} (T_{s,i} - T_{a,i}) + L_v h_{M,i} (\rho_{ve,s,i} - \rho_{ve,a,i}) - \alpha_i \Phi_{ray,i} \quad (8)$$

Mass density of dry hemp concrete material ρ_0 is 415 Kg/m³. Its thermal conductivity is related to moisture content:

$$\lambda = 0.1058 + 0.77 \theta \quad (9)$$

A. Determination of transport coefficients

Hemp concrete transport coefficients were calculated using relations suggested by Philip et al. [19] and Kunzel [21]. For the transport coefficient associated to a gradient of moisture content, it is computed from dry vapour permeability δ_0 (kg.m⁻¹.s⁻¹.Pa⁻¹) ($\delta_0 = \frac{\delta_a}{\mu}$ where δ_a is air vapour permeability which is equal to 2.10⁻¹⁰ kg.m⁻¹.s⁻¹.Pa⁻¹ at 23°C and μ is material vapour diffusion resistance factor) and the specific hygric capacity ξ which is the slope of moisture retention curve:

$$D_\theta = \frac{\delta_a}{\mu} \frac{P_{vs}}{\rho_s} \frac{1}{\xi} \quad (10)$$

Vapour transport coefficient under a temperature gradient is given by the relation:

$$D_{T,ve} = \varphi \frac{\delta_a}{\rho_l \mu} \frac{dP_{vs}}{dT} \quad (11)$$

To simplify the problem, vapour transport coefficient under moisture gradient is assumed equal to moisture transport coefficient under moisture gradient:

$$D_{\theta,ve} = D_\theta \quad (12)$$

Thermomigration of liquid phase is also neglected and thus thermomigration coefficient D_T is also equal to $D_{T,ve}$.

B. Sorption isotherm

In this study we use the analytical model of adsorption/desorption proposed by Merakeb [15]. In this model, the relation between the water content and the relative humidity is written in the form:

$$\ln \left(\frac{\theta}{\theta_s} \right) = a \cdot \ln(\phi) \cdot \exp(b\phi) \quad (13)$$

Where a and b are parameters determined experimentally.

Referring to [4] and [5], hemp concrete sorption curves are determined for values of relative humidity varying from 0 to 100%.

For the adsorption curve (from 0 to 100%):

$$\theta = 0,151 \cdot \exp[1,1 \cdot \ln(\phi) \cdot \exp(2,3 \cdot \phi)] \quad (14)$$

For the desorption curve (from 100% to 0%):

$$\theta = 0,151 \cdot \exp[0,75 \cdot \ln(\phi) \cdot \exp(2,3 \cdot \phi)] \quad (15)$$

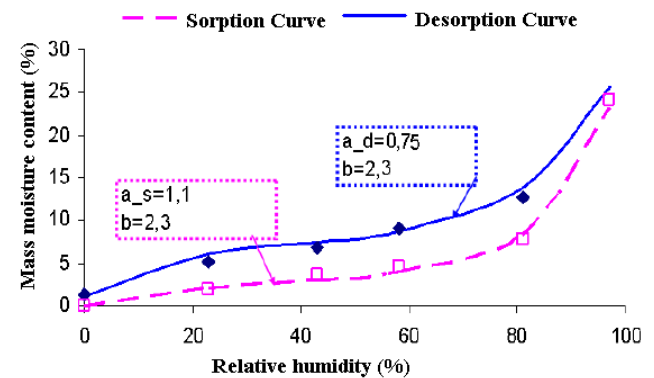


Fig. 4 : Comparison between analytical (Merakeb formulation) and experimental sorption and desorption curves (Collet data) of hemp-lime mixture when varying relative humidity from 0 to 100%.

Fig. 4 shows hemp concrete adsorption and desorption curves. In the general case, between these two curves, the sorption curve is given by :

$$\ln\left(\frac{\theta}{\theta_s}\right) = a \cdot \ln(\phi) \cdot \exp(b \cdot \phi) + \Delta a \cdot \ln(\phi) \cdot \exp(\Delta b \cdot \phi) \quad (16)$$

Δa and Δb are defined by equations that depend on the sorption state (whether it is adsorption or desorption).

IV. SIMULATIONS FOR THE FIRST EXPERIMENT CASE

To solve the previous system of equations we used the Simulation Problem Analysis and Research Kernel (SPARK), a simulation environment allowing to solve efficiently differential equation systems [22]-[25]. Equations (2) and (5) are discretized using the finite difference method.

We compared simulation results with experimental data for the specimen 1. Two cases are considered with and without taking into account sorption hysteresis.

Fig. 5 compares numerical results with hysteresis to experimental data. It can be seen that there is a good agreement between both curves.

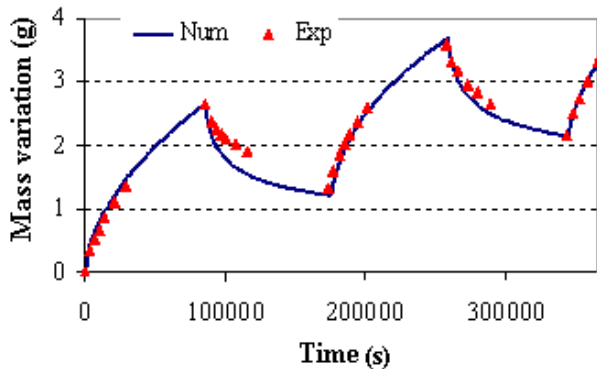


Fig. 5 Comparison between numerical and experimental data for specimen 1.

Fig. 6 shows mass variation when neglecting sorption hysteresis. Three cases are considered: taking the adsorption curve as the sorption isotherm, taking the desorption curve or taking the mean curve between the adsorption and desorption. We notice that none of the three cases is in agreement with the dynamical variation of the specimen mass variation.

Fig. 7 compares moisture content in the material at 6 mm depth from the surface with and without hysteresis. It can be seen that for the model using hysteresis the curve tends toward the model neglecting hysteresis and using the mean curve between adsorption and desorption. However, as shown in Fig. 7, mass variation of specimen for the two cases is different. This is mainly due to initial moisture content which is different for both cases.

Fig. 8 shows specimen mass variation for a period of two weeks with and without sorption hysteresis. When neglecting hysteresis, periodic variation is reached after 4 days whereas it needs two weeks to reach equilibrium when sorption hysteresis is considered. These results are in agreement with

those found in literature for a hemp concrete with similar properties [26].

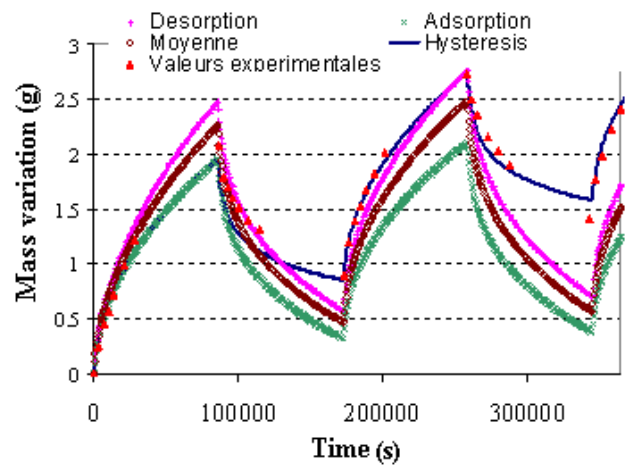


Fig. 6. Comparison between numerical and experimental data when neglecting hysteresis.

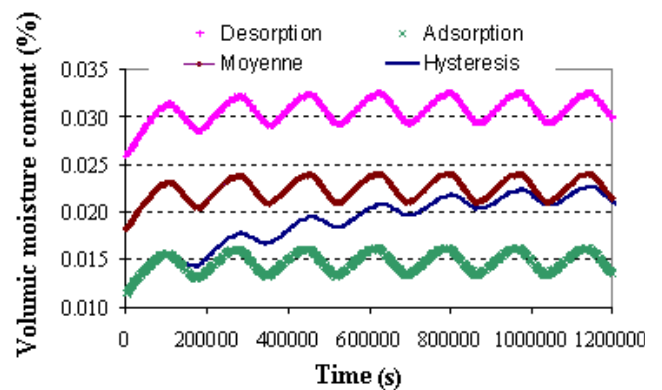


Fig. 7. Moisture content variation at 6mm depth for the 4 sorption isotherm cases and for a period of two weeks.

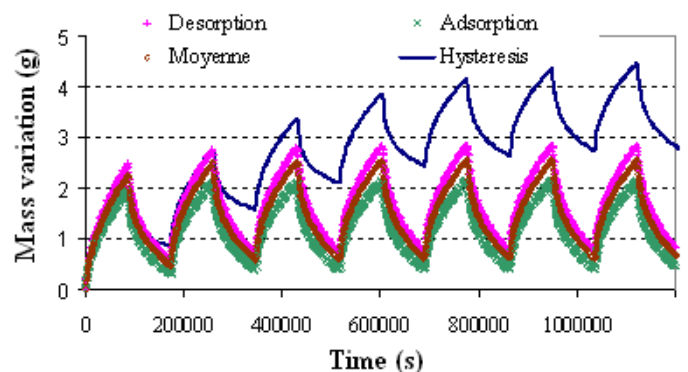


Fig. 8. Specimen mass variation for a period of two weeks with and without sorption hysteresis.

V. SIMULATIONS FOR THE SECOND EXPERIMENT CASE

Fig. 9 shows specimen mass variation under a relative humidity static step of 71% for a period of 24 hours for both experimental and numerical cases. A good agreement is shown. The difference between both cases at the end of the adsorption phase is 0.17 g which is about 4.8%. At the end of the desorption phase the difference is about 0.03 g (3.2% difference).

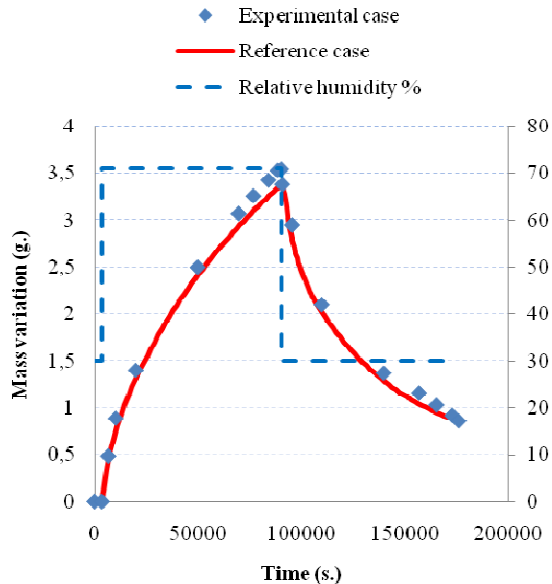


Fig. 9 : Comparison between numerical and experimental results for the second case experimentation

Running simulation for a specimen of 3.75 cm thickness and comparing comparing results with data given in [14] for gypsum we notice that hemp concrete has a very higher moisture buffering capacity. Fig. 10 shows mass variation for both cases. Hemp concrete mass increases 2.54 g whereas gypsum board mass increases 0.68 g which is 74% lower. At the end of the test, hemp concrete mass decreases to 0.89 g meaning it rejects about 1.65 g of moisture while gypsum rejects 0.47 g under the same conditions.

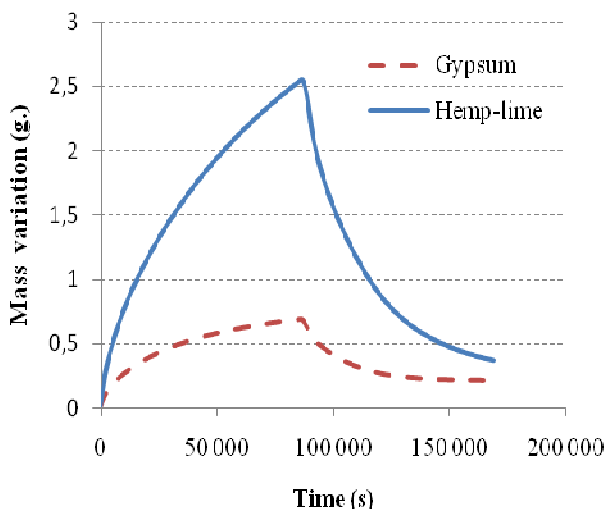


Fig. 10 : Comparison between numerical results for hemp concrete and gypsum board for the same conditions and thickness.

These results are also in accordance with results obtained by Woloszyn et al. [27]. After 10h and under a static step of 75% of relative humidity, gypsum mass increases about 26 g/m². Under the same conditions, mass growth in hemp concrete would be 118 g/m². For 1 cm of brick, mass growth is about 19 g/m² confirming high moisture buffering capacity of hemp concrete.

VI. PARAMETRIC STUDY

To better understand the influence of each parameter of the physical model on the results, a sensitivity analysis is done in this part. The studied case is the case of the experiment 2 and is called reference case. Parameters considered are material thickness, its surface area exposed to air, vapour permeability, mass convection coefficient, hysteresis phenomenon and sorption isotherm curves.

A. Effect of material thickness

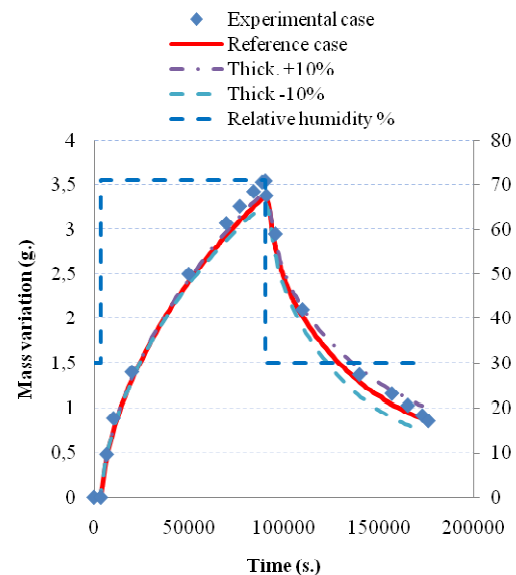


Fig. 11 : Effect of varying material thickness of 10% on moisture uptake.

Fig. 11 shows the effect of material thickness on moisture mass uptake variation. As material thickness increases moisture uptake increases. Compared to reference case, after 24h moisture uptake increases about 0.05 g which is about 1.5%. When thickness decreases 10%, moisture uptake decreases about 0.08 g or 2.4 %. Thickness variation has little impact in this case because material thickness is higher than moisture penetration depth defined by equation (1). At the end of desorption phase, mass variation decreases and in both cases the difference with the reference case is about 0.14 g meaning that when material thickness increases, the whole mass of rejected water is 2.4 g and when thickness decreases the whole mass rejected is 2.54 g whereas for the reference case rejected mass is 2.47 g. When material thickness increases more water will penetrate through the material, the pores get more filled and when water is rejected during desorption its motion is slowed due to the existence of ink-bottle shaped pores [12] thus it rejects less water.

B. Effect of exposed surface area

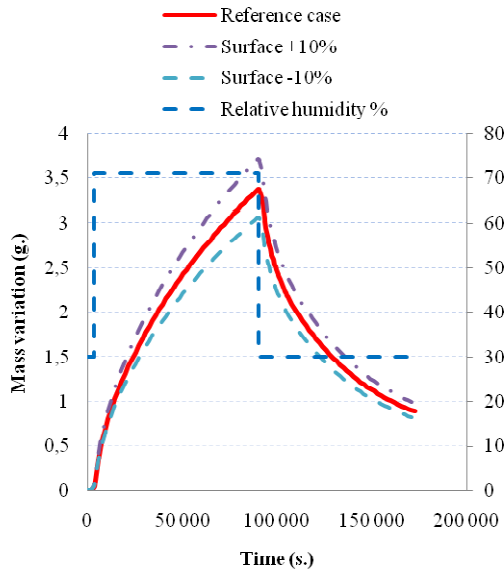


Fig. 12 : Effect of varying 10% material exposed surface area.

Fig. 12 shows the effect of varying material exposed surface. In this case, mass variation is directly proportional to the surface. When surface increases 10%, mass variation increases 10% and vice versa.

C. Effect of material vapour permeability

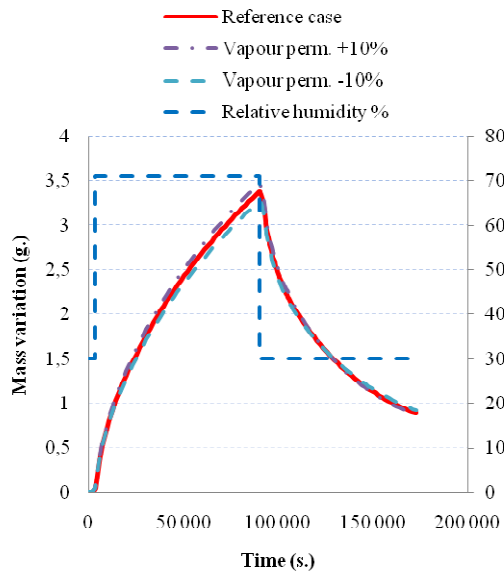


Fig. 13 : Variation of moisture uptake when material vapour permeability varies 10%.

Fig. 13 shows the variation of moisture uptake when material vapour permeability δ_0 varies of 10%. Increasing the vapour permeability leads to a growth in material vapour diffusivity and thus more moisture is adsorbed and desorbed and vice versa. Incrementing permeability of 10%, leads to an increment of moisture uptake of 2.7 %. Decreasing permeability 10%, decreases moisture uptake about 3%. In desorption phase, material rejects 2.6 g (+5.2%) of moisture when permeability increases and 2.35g (-4.9%) when it decreases.

D. Effect of mass convection coefficient

Increasing mass convection coefficient 10% leads to a growth in moisture uptake of almost 2% and moisture rejection of 2.8% and vice versa.

E. Effect of neglecting hysteresis phenomenon

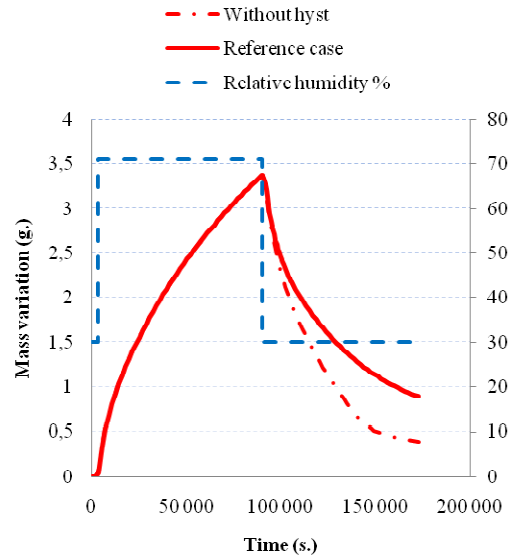


Fig. 14 : Effect of neglecting hysteresis phenomenon on specimen mass variation.

Fig. 14 shows the effect of neglecting hysteresis phenomenon on moisture uptake. During the adsorption phase both cases are identical but during desorption the two curves are separated and neglecting hysteresis tends to surestimate rejected moisture mass (2.97 g instead of 2.47 g which is 20% higher).

F. Effect of isotherm curves variation

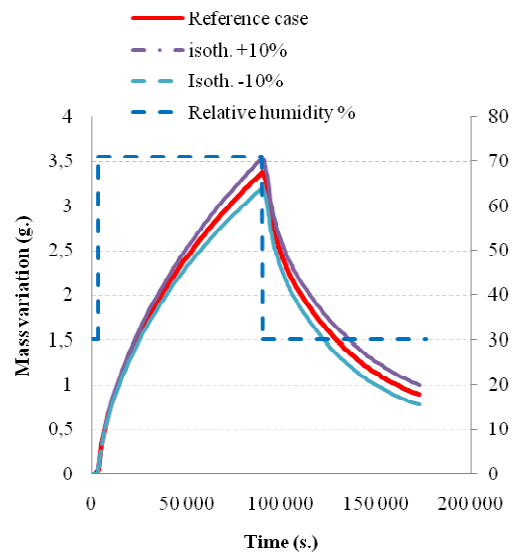


Fig. 15 : Effect of varying 10% material exposed surface area.

Fig. 15 shows effect of varying 10% isotherm curves or exactly the term θ_s in the equation 13 for the sorption and desorption curves. It can be seen that as isotherm curves are higher, material moisture content tends to increase at the same relative humidity level and thus moisture uptake will increase. Increasing θ_s 10%, increases moisture uptake 4.7% and decreasing it 10% decreases moisture content 5%. For both cases rejected moisture mass during desorption is about 2.5 different than reference case.

So we notice that the main parameters affecting moisture uptake or rejection are hysteresis phenomenon, isotherm curve, material exposed surface, vapour permeability finally material thickness.

VII. CONCLUSION

In this paper, we investigated experimentally and numerically the hydric behaviour of a mixture of hemp and lime (hemp concrete) under periodical static step change of air relative humidity. Compared to gypsum and brick, our results suggest that hemp concrete has a higher moisture buffering capacity. In parallel a numerical model using the simulation environment SPARK showed the importance of taking into account sorption isotherm hysteresis in order to predict material dynamical behaviour. A parametrical study has shown that the most important parameters affecting moisture uptake and rejection are hysteresis phenomenon, material sorption curves, its air exposed surface and vapour permeability. These results are actually completed with experimental data for longer periods.

NOMENCLATURE

Symbol	Definition	Unit
C	Specific heat	$\text{J kg}^{-1} \cdot \text{K}^{-1}$
C_0	Specific heat of dry material	$\text{J kg}^{-1} \cdot \text{K}^{-1}$
C_1	Specific heat of water	$\text{J kg}^{-1} \cdot \text{K}^{-1}$
D_T	Mass transport coefficient associated to a temperature gradient	$\text{m}^2 \cdot \text{s}^{-1} \cdot \text{°C}^{-1}$
$D_{T,v}$	Vapor transport coefficient associated to a temperature gradient	$\text{m}^2 \cdot \text{s}^{-1} \cdot \text{°C}^{-1}$
D_θ	Mass transport coefficient associated to a moisture content gradient	$\text{m}^2 \cdot \text{s}^{-1}$
$D_{\theta,v}$	Vapor transport coefficient associated to a moisture content gradient	$\text{m}^2 \cdot \text{s}^{-1}$
d	Moisture penetration depth	m
G	Gravity acceleration	$\text{m}^2 \cdot \text{s}^{-1}$
h_M	Mass transfer convection coefficient	$\text{kg} \cdot \text{m}^{-2} \cdot \text{s}^{-1}$
h_T	Heat transfer convection coefficient	$\text{W} \cdot \text{K}^{-1} \cdot \text{m}^{-2}$
L_v	Heat of vaporization	$\text{J} \cdot \text{kg}^{-1}$
T	Temperature	°C
t	Time	s
α	Solar radiation absorption coefficient	
θ	Moisture content	$\text{m}^3 \cdot \text{m}^{-3}$
λ	Thermal conductivity	$\text{W} \cdot \text{m}^{-2} \cdot \text{K}^{-1}$
ρ_0	Mass density of dry material	$\text{kg} \cdot \text{m}^{-3}$
ρ_l	Mass density of water	$\text{kg} \cdot \text{m}^{-3}$
ρ_v	Mass density of vapor water	$\text{kg} \cdot \text{m}^{-3}$

REFERENCES

- [1] J.L. Cnaletti, G. Notton, A. Damian, I. Colda, C. Cristofari. "New concept of solar air heater integrated in the building". 4th IASME/WSEAS International Conference on Energy, Environment, Ecosystems and Sustainable Development, Algarve, Portugal, pp. 52-59, 2008.
- [2] S. Bica, L. Roşiu, R. Radoslav. "What characteristics define ecological building materials?"; *Proceedings of the 7th IASME/WSEAS International Conference on Heat Transfer Thermal Engineering & Environment*, Moscow, pp. 159-164, 2009.
- [3] A. Shea, M. Lawrence, P. Walker, Hygrothermal performance of an experimental hemp-lime building, *Construction and Building Materials*, 36, p. 270-275, 2012.
- [4] V. Cerezo, "Propriétés mécaniques, thermiques et acoustiques d'un matériau à base de particules végétales : approche expérimentale et modélisation théorique", PhD, INSA & ENTPE de Lyon, p. 242, 2005.
- [5] F. Collet, "Caractérisation hydrique et thermique de matériaux de génie civil à faibles impacts environnementaux", PhD, INSA de Rennes, p. 220, 2004.
- [6] S. Elfordy, F. Lucas, F. Tancret, Y. Scudeller, L. Goudet. Mechanical and thermal properties of lime and hemp concrete (« hempcrete ») manufactured by a projection process, *Construction and Building Materials*, 22(10), p. 2116-23, 2008.
- [7] F. Murphy, S. Pavia, R. Walker, an assessment of the physical properties of lime-hemp concrete, Proc. of BRI/CRI. Ní Nualláin, Walsh, West, Cannon, Caprani, McCabe eds. Cork 2010.
- [8] D. Sedan, C. Pagnoux, A. Smith, T. Chotard, T., 'Mechanical properties of hemp fibre reinforced cement: Influence of the fibre/matrix interaction', *Journal of the European Ceramic Society*, 28, 183-192, 2008.
- [9] P.B. de Bruijn, K.H. Jeppsson, K. Sandin, C. Nilsson, 'Mechanical properties of lime-hemp concrete containing shives and fibres', *Biosystems Engineering*, 103, 474-479, 2009.
- [10] M. Le Troëdec, C.S., Peyratout, T. Chotard, J.P. Bonnet, A. Smith, R. Guinebrière, 'Physico-chemical modifications of the interactions between hemp fibres and a lime mineral matrix: impacts on mechanical properties of mortars', *Journal of the European Ceramic Society*, 29, 10, 1861-1868, 2009.
- [11] L. Arnaud, Mechanical and thermal properties of hemp mortars and wools: experimental and theoretical approaches, Bioresource Hemp 2000 & other fibre crops, Wolfsburg. Nova Institut, Hürth, Germany.
- [12] F. Collet, M. Bart, L. Serres, J. Miriel, Porous structure and water vapour sorption of hemp-based materials, *Construction and Building Materials*, 22, 1271-80, 2008.
- [13] A.D. Tran Le, C. Maalouf, T.H. Mai, E. Wurtz, F. Collet Transient hygrothermal behaviour of a hemp concrete building envelope. *Energy and Buildings*, vol. 42, p. 1797-1806, 2010.
- [14] N. Mendes Models for prediction of heat and moisture transfer through porous building element, Thèse de doctorat, 225, Federal University of Santa Catarina, Florianopolis, SC, Brésil, 1997.
- [15] S. Merakeb, F. Dubois, C. Petit, Modeling of the sorption hysteresis for good. *Wood Sci Technol*, 2009, vol.43, 575-589.
- [16] C. James, C.J. Simonson, P. Talukdar, S. Roels, Numerical and experimental data set for benchmarking hygroscopic buffering models. *International Journal of Heat and Mass Transfer* 53 (19-20), 3638-3654, 2010.
- [17] J. Arfvidsson, Moisture penetration for periodically varying relative humidity at boundary, *Acta Physica Aedificiorum*, vol. 2, 1999.
- [18] A.D. Tran Le, Etude des transferts hygrothermiques dans le béton de chanvre et leur application au bâtiment, PhD thesis, Université de Reims Champagne Ardenne, , November 2010 (in French).
- [19] J.R. Philip, and D.A. De Vries, Moisture movement in porous materials under temperature gradients, *Transaction of American Geophysical Union*. V.38, n.2, p.222-232, 1957.
- [20] C.R. Pedersen., "Prediction of moisture transfer in building constructions", *Building and Environment* (3) 387-397, 1992.
- [21] M. Kunzel Simultaneous heat and moisture transport in building components, Fraunhofer Institute of building physics, Germany, 1995;
- [22] A.D. Tran le., C. Maalouf , K.C. Mendonça, T.H. Mai, E. Wurtz , " Study of moisture transfer in doubled-layered wall with imperfect thermal and hydraulic contact resistances", *Journal of Building Performance Simulation*; 2: 251-266, 2009.
- [23] C. Maalouf, E. Wurtz, L. Mora, "Effect of Free Cooling on the Operation of a Desiccant Evaporative Cooling System", *International Journal of Ventilation*, vol. 7, pp. 125-138, 2008.
- [24] C. Maalouf, A. D. Tran Le, M. Lachi, E. Wurtz, T. H. Mai, Effect of moisture transfer on thermal inertia in simple layer walls. Case of a vegetal fiber material. *International Journal of Mathematical Models and Methods in Applied Sciences* vol 5 (6), pp 1127-1134, 2011
- [25] C. Maalouf, A. D. Tran Le, M. Lachi, E. Wurtz, T. H. Mai, Effect of moisture transfer on thermal inertia in simple layer walls. Case of a

vegetal fiber material. International Journal of Mathematical Models and Methods in Applied Sciences vol 5 (1), pp 33-47,2011

- [26] A. Evrard . Transient hygrothermal behaviour of Lime- Hemp materials. Thèse de doctorat de sciences de l'ingénieur, Ecole polytechnique de Louvain Unité d'Architecture, 2008.
- [27] M. Woloszyn, M. May, J. Kwiatkowski, Influence des conditions aux limites sur les mesures de « l'inertie hygrique » des matériaux de construction, *24èmes Rencontres Universitaires de Génie Civil*, La Grande Motte, 2006.